

LETTERS

Messenger RNA targeting to endoplasmic reticulum stress signalling sites

Tomás Aragón^{1,2*}, Eelco van Anken^{1,2*}, David Pincus^{1,2}, Iana M. Serafimova^{1,2}, Alexei V. Korenykh^{1,2}, Claudia A. Rubio^{1,2} & Peter Walter^{1,2}

Deficiencies in the protein-folding capacity of the endoplasmic reticulum (ER) in all eukaryotic cells lead to ER stress and trigger the unfolded protein response (UPR)^{1–3}. ER stress is sensed by Ire1, a transmembrane kinase/endoribonuclease, which initiates the non-conventional splicing of the messenger RNA encoding a key transcription activator, Hac1 in yeast or XBP1 in metazoans. In the absence of ER stress, ribosomes are stalled on unspliced *HAC1* mRNA. The translational control is imposed by a base-pairing interaction between the *HAC1* intron and the *HAC1* 5' untranslated region⁴. After excision of the intron, transfer RNA ligase joins the severed exons^{5,6}, lifting the translational block and allowing synthesis of Hac1 from the spliced *HAC1* mRNA to ensue⁴. Hac1 in turn drives the UPR gene expression program comprising 7–8% of the yeast genome⁷ to counteract ER stress. Here we show that, on activation, Ire1 molecules cluster in the ER membrane into discrete foci of higher-order oligomers, to which unspliced *HAC1* mRNA is recruited by means of a conserved bipartite targeting element contained in the 3' untranslated region. Disruption of either Ire1 clustering or *HAC1* mRNA recruitment impairs UPR signalling. The *HAC1* 3' untranslated region element is sufficient to target other mRNAs to Ire1 foci, as long as their translation is repressed. Translational repression afforded by the intron fulfils this requirement for *HAC1* mRNA. Recruitment of mRNA to signalling centres provides a new paradigm for the control of eukaryotic gene expression.

In vitro studies indicate that the information required for *HAC1* mRNA splicing is confined to the intron and the regions surrounding the splice junctions⁸. Surprisingly, *in vivo* splicing of *HAC1* mRNA was greatly diminished when its 3' untranslated region (3' UTR) was replaced by the 3' UTRs of other yeast mRNAs, such as that of actin (*ACT1*, Fig. 1b) or 3-phosphoglycerate kinase (*PGK1*, data not shown). Consistent with this finding, cells bearing a chimaeric *HAC1* gene with the 3' UTR of *ACT1*, *HAC1*-3'*act1*, expressed Hac1 protein at trace levels that were too low to mount a functional UPR and failed to grow in ER stress conditions (Fig. 1b). Thus, the *HAC1* 3' UTR harbours an element important for *HAC1* mRNA splicing *in vivo*.

Mutational probing experiments (not shown) indicate that the *HAC1* 3' UTR contains a prominent, extended stem-loop (Fig. 1c). Interestingly, two short sequence motifs within the stem-loop are highly conserved among all *HAC1* orthologues identified; eight representatives are shown in Fig. 1d. The sequence motifs map to opposite strands and are juxtaposed in the distal part of the stem, constituting a 3' UTR bipartite element (3' BE; Fig. 1c, 3' BE in red).

To assess the importance of the 3' BE for *HAC1* mRNA splicing *in vivo*, we used a splicing reporter in which we replaced the first 648 nucleotides of the *HAC1* coding sequence in the first exon with that of green fluorescent protein (GFP; Fig. 1a, green bar). This reporter

allowed us to monitor the effect of 3' UTR mutations on mRNA splicing in cells that can mount a functional UPR, sustained by endogenous *HAC1* mRNA. The splicing reporter mRNA was efficiently spliced on UPR induction. In contrast, splicing was greatly diminished when the 3' BE was deleted (Δ 3' BE, Fig. 1e). Consistent with these results, deletion of the 3' BE in *HAC1* severely reduced *HAC1* mRNA splicing and impaired cell survival under ER stress conditions (Fig. 1e). Only residual splicing of endogenous *HAC1* mRNA occurred in the absence of the 3' BE, indicating that the 3' BE accounts in large part for the contribution of the 3' UTR to *HAC1* mRNA splicing. Insertion of a 64-nucleotide 3' UTR fragment containing the central portion of the stem including the 3' BE (Fig. 1d, enlarged on right) into the splicing reporter bearing the *ACT1* 3' UTR restored splicing greatly (Fig. 1f).

To test whether the 3' UTR affects the ability of Ire1 endonuclease to bind or catalyse the cleavage of *HAC1* mRNA, we reconstituted the intron excision reaction *in vitro*. Ire1 cleaved *HAC1* mRNA with the same rate in the presence or absence of the 3' BE (Fig. 1g). Thus, the 3' BE is not required for splicing *in vitro*.

The importance of the 3' BE for *HAC1* mRNA splicing *in vivo* indicated that it may serve to target the mRNA to sites in the cell where splicing takes place. To test this notion, we visualized Ire1 protein and *HAC1* mRNA *in vivo*, using the imaging constructs depicted in Fig. 2a. For Ire1, we inserted a GFP or mCherry into the cytosolic portion of Ire1 adjacent to its transmembrane region. For *HAC1* mRNA, we inserted 16 copies of a U1A binding site into the 3' UTR downstream of the 3' BE. The mRNA can then be visualized by co-expression of a GFP-tagged U1A-RNA-binding protein that docks to the U1A binding sites⁹. Both Ire1 and *HAC1* mRNA imaging constructs fully restored growth of *ire1* Δ and *hac1* Δ (Fig. 2b) cells under ER stress. In the absence of stress, Ire1–GFP co-localized with the ER marked by Sec63–mCherry (Fig. 2c). Most *HAC1*^{U1A} mRNA displayed a grainy signal dispersed throughout the cytosol (Fig. 2d), with a fraction of *HAC1* mRNA signal also found at the ER in agreement with previous observations¹⁰.

Induction of ER stress notably altered the localization of both Ire1 and *HAC1* mRNA. Most Ire1 (82 \pm 6%; see Methods) clustered into distinct foci localized both to the nuclear envelope and to the cortical ER (Fig. 2c–e), in agreement with recent observations¹¹. *HAC1* mRNA strongly co-localized (co-localization index (CI) of 56 \pm 10; see Methods, Fig. 2e) with Ire1 in foci (Fig. 2d, arrowheads). This recruitment is specific, because control *PGK1*^{U1A} mRNA remained dispersed in the cytosol under ER stress conditions (Fig. 2f).

Clustering of mRNAs in cytosolic foci is not unprecedented. Several stresses, such as nutrient starvation, cause aggregation of untranslated mRNAs into processing bodies (P-bodies) where they are stored and/or degraded¹². The Ire1/*HAC1* mRNA clusters, however, are distinct

¹Department of Biochemistry and Biophysics, and ²Howard Hughes Medical Institute, University of California at San Francisco, San Francisco, California 94158-2517, USA.

*These authors contributed equally to this work.

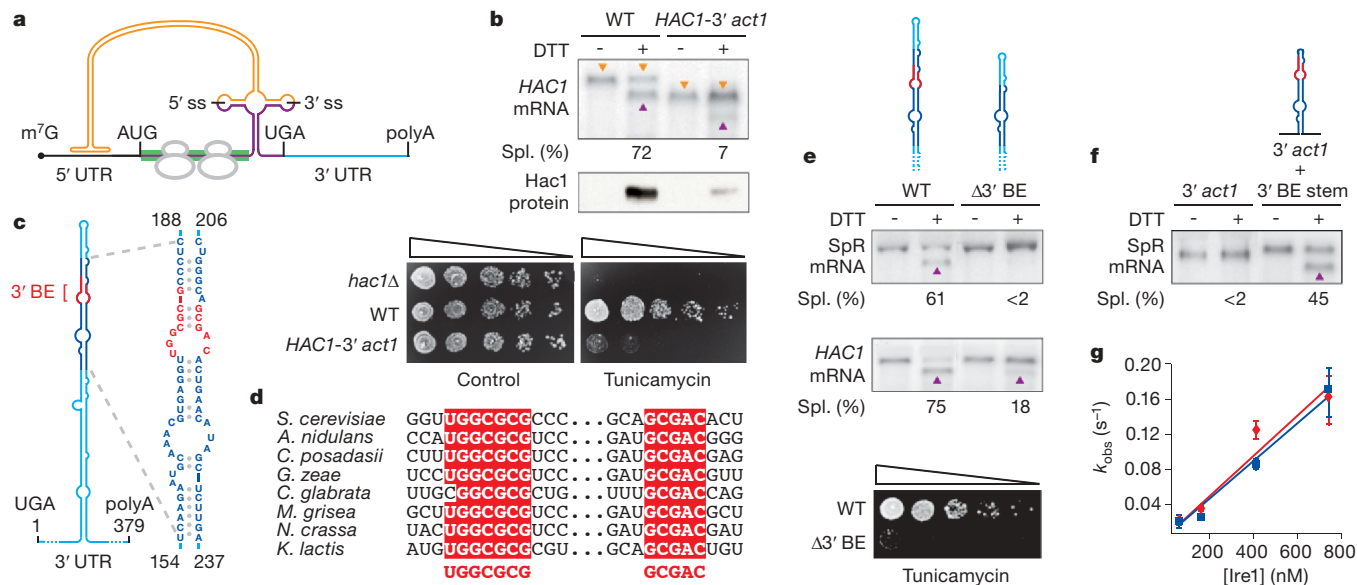


Figure 1 | A conserved element in the 3' UTR of *HAC1* mRNA is required for splicing *in vivo*, but not *in vitro*. **a**, Schematic of *HAC1* mRNA. The *HAC1* open reading frame (ORF) is divided into two exons (purple). The intron (orange) base pairs with the 5' UTR (black), causing stalling of ribosomes (grey). Ire1 cleaves the intron at the indicated splice sites (5' ss and 3' ss). The green bar depicts where the GFP ORF replaces the *HAC1* sequence in the splicing reporter. The 3' UTR is indicated in light blue. The 5' cap (m⁷G), start codon (AUG), stop codon (UGA) and polyadenylation signal (polyA) are indicated. **b**, **e**, **f**, Northern blot of *HAC1* or splicing reporter (SpR) mRNA variants before or after ER stress induction with DTT (10 mM) for 45 min. Purple triangles denote spliced mRNAs; orange triangles denote unspliced mRNAs (only in **b**). Percentage mRNA splicing (Spl. (%)) is indicated. Yeast strains harbour: a genomic *HAC1* copy with its own (WT) or *ACT1*'s 3' UTR sequence (*HAC1*-3' *act1*; **b**, top); a genomic copy of SpR (**e**, top) or *HAC1* (**e**, middle) bearing either the wild-type (WT) or the $\Delta 3'$ BE mutant 3' UTR of *HAC1*, as depicted; or a genomic copy of SpR with the 3' UTR of *ACT1* with (3' *act1* + 3' BE stem) or without (3' *act1*) an insertion

of the 64-nucleotide element (shown in expanded view in **c**), as depicted (**f**). **b**, Middle: western blot of haemagglutinin (HA)-tagged Hacl1 protein from lysates from strains as in the top panel of **b**. **e**, Viability assay by 1:5 serial dilutions of *hac1* Δ or strains as in the top panel of **b** or the middle panel of **e**, spotted onto solid media with or without 0.2 $\mu\text{g ml}^{-1}$ of the ER-stress-inducer tunicamycin. Plates were photographed after 3 days growing at 30 °C. **c**, Schematic of the *HAC1* 3' UTR stem-loop structure with the 3' BE (red) in a region (dark blue) that is shown in expanded view to the right; positional numbering is from UGA stop codon. **d**, Alignment of the 3' BE in *HAC1* homologues (*Saccharomyces cerevisiae*, *Aspergillus nidulans*, *Coccidioides posadasii*, *Gibberella zeae*, *Candida glabrata*, *Magnaporthea grisea*, *Neurospora crassa*, *Kluyveromyces lactis*). **g**, An *in vitro* intron excision reaction was performed as described⁸ with Ire1 concentrations (50 nM, 150 nM, 400 nM and 730 nM) of wild-type (red diamonds) or $\Delta 3'$ BE (blue squares) *HAC1* mRNA as substrates. Error bars show standard errors of single-exponential fitting.

from P-bodies: on glucose depletion *HAC1* mRNA did cluster into P-bodies marked by Lsm1–mCherry¹³. In contrast, under ER stress conditions Lsm1–mCherry did not co-localize with *HAC1* mRNA foci but remained dispersed throughout the cytosol (Fig. 2g). Thus, the Ire1/*HAC1* mRNA foci constitute previously unknown sites of mRNA clustering in the cytosol that are specific for the UPR.

We next determined the role of each of the three key UPR players—Ire1, *HAC1* mRNA and tRNA ligase—in organizing the foci. In *rlg1-100* cells bearing mutant tRNA ligase defective in UPR signalling⁵, co-clustering of Ire1 and *HAC1* mRNA occurred normally (Fig. 2h). This result is consistent with the fact that cleavage of *HAC1* mRNA by Ire1 is not dependent on the subsequent ligation step⁵. Likewise, *HAC1* mRNA was not required for Ire1 clustering, because Ire1–GFP formed foci in *hac1* Δ cells (Fig. 2h and ref. 11). Conversely, *HAC1* mRNA failed to form foci in *ire1* Δ cells (Fig. 2h). Thus, clustering of Ire1 in response to ER stress is epistatic to *HAC1* mRNA clustering.

Having established that *HAC1* mRNA is targeted to Ire1 foci in an ER-stress-driven manner, we assessed the role of the 3' UTR of *HAC1* mRNA in the process. To this end, we added the U1A visualization module to the splicing reporter used in Fig. 1e (SpR^{U1A}). The SpR^{U1A} mRNA containing a wild-type *HAC1* 3' UTR co-localized with Ire1–mCherry in foci (CI: 64 \pm 20; Fig. 2i). In contrast, co-localization with Ire1 foci of the SpR^{U1A} mRNA lacking the 3' BE was minimal (CI: 4 \pm 6; Fig. 2i), at levels comparable to the control *PGK1*^{U1A} mRNA (CI, 3 \pm 4). Thus, the stem-loop structure in the 3' UTR of *HAC1* mRNA—with the 3' BE at its core—indeed serves as a

targeting element that guides *HAC1* mRNA to Ire1 foci to allow splicing *in vivo* and cell survival under ER stress.

We next followed a time course of foci formation and downstream signalling on induction of ER stress. Clustering of Ire1 into foci and recruitment of *HAC1* mRNA (Fig. 3a, b) or of SpR^{U1A} mRNA (Supplementary Fig. 1) into these foci correlated well with the onset of *HAC1* mRNA splicing and Hacl1 protein production (Fig. 3c). These findings show that Ire1 and *HAC1* mRNA clustering is geared to transduce ER stress rapidly. Under conditions in which ER stress builds up more gradually, the encounter of Ire1 and *HAC1*^{U1A} mRNA in foci likewise paralleled the signalling response, but at a slower pace (Supplementary Fig. 2). The synchronicity of Ire1/*HAC1* mRNA clustering and downstream signalling events underscores that the foci constitute functional mRNA-splicing centres.

Ire1 clusters in only ~3–10 foci per cell. Because yeast contains ~200–300 molecules of Ire1 per cell¹⁴, the foci are composed of a few tens of Ire1 molecules each, indicating that the foci harbour higher-order oligomers of Ire1. From the crystal structure of the Ire1 ER-luminal domain, we identified two separate dimerization interfaces, both of which are essential for optimal UPR signalling, indicating that oligomerization is important for cells to mount a robust UPR¹⁵ (Fig. 3d). Accordingly, simultaneous disruption of both interfaces notably reduced *HAC1* mRNA splicing and cell growth under ER stress conditions, whereas the single-interface disruptions, which still can form Ire1 dimers by means of one interface, displayed intermediate splicing and growth phenotypes (Fig. 3e). Disruption of either interface prevented foci formation (Fig. 3f, Supplementary Fig. 3 and

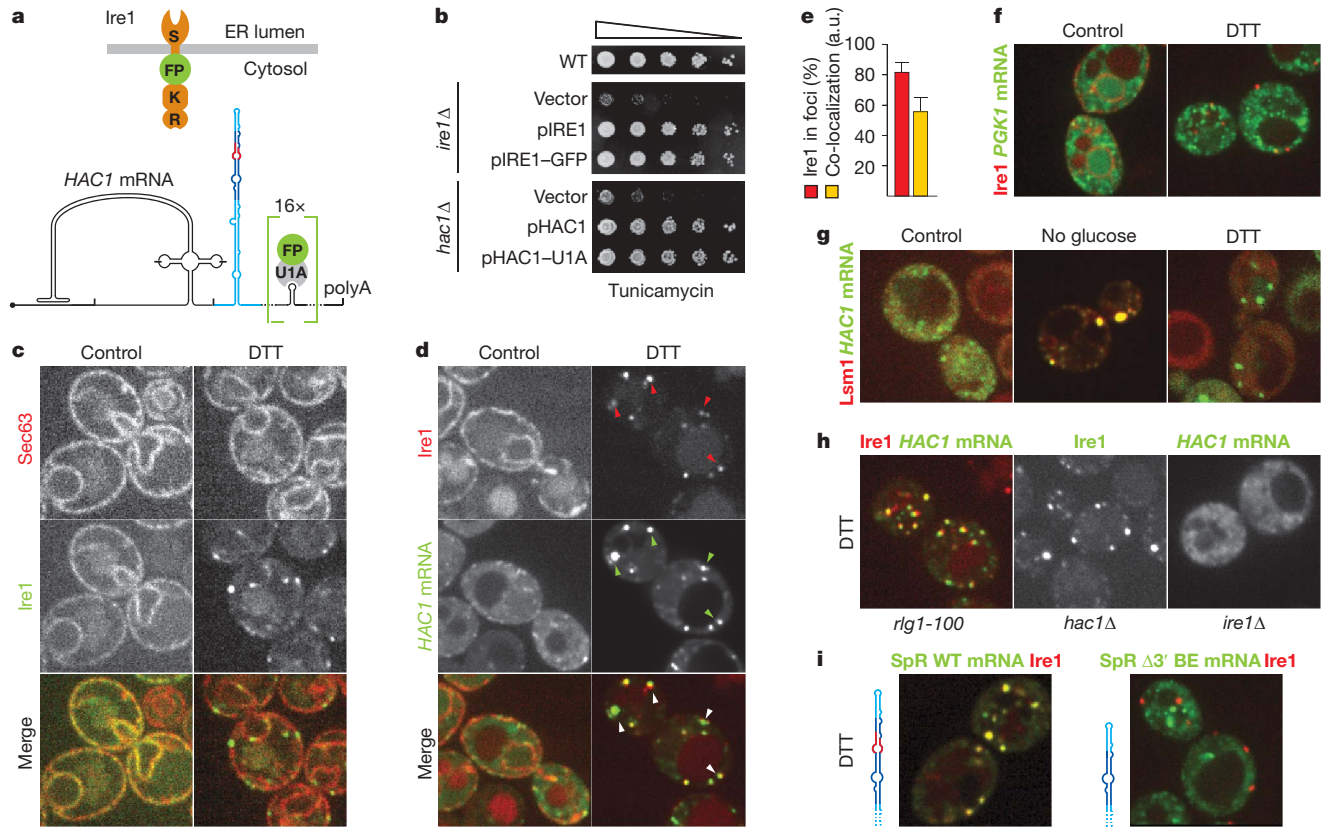


Figure 2 | In response to ER stress *HAC1* mRNA localizes to Ire1 foci in a 3' BE-dependent manner. **a**, Schematic of Ire1 and *HAC1* mRNA imaging constructs: Ire1 has an ER-luminal stress-sensing domain (S), and has a kinase (K) and an endoribonuclease domain (R) at its cytosolic face. GFP or mCherry (FP) was inserted between the transmembrane region and the kinase domain. 16 U1A binding sites were inserted into the 3' UTR of *HAC1* mRNA downstream of the stem-loop. Binding of GFP-tagged U1A protein allows visualisation of the mRNA. **b**, Viability assay under ER stress conditions ($0.2 \mu\text{g ml}^{-1}$ tunicamycin) of wild-type (WT) or *ire1* Δ yeast complemented with empty vector or with centromeric plasmids bearing a wild-type (pIRE1) or the GFP-tagged imaging copy of Ire1 (pIRE1-GFP; top), or of *hac1* Δ yeast complemented with either empty plasmid or with a 2- μm plasmid bearing a wild-type (pHAC1) or the U1A-tagged imaging copy of *HAC1* (pHAC1-U1A; bottom). **c**, **d**, Localization of Sec63-mCherry and Ire1-GFP (**c**) or Ire1-mCherry and *HAC1*^{U1A} mRNA decorated with U1A-GFP (**d**) before (left panels, control) and after (right panels, DTT)

induction of ER stress. Arrowheads in **d** denote Ire1/*HAC1* mRNA foci. **e**, Histogram depicting the percentage of Ire1 signal in foci (red bar) and the co-localization index for *HAC1*^{U1A} mRNA recruitment into Ire1 foci expressed in arbitrary units (yellow bar); means and s.e.m. are shown, $n = 9$. **f**, Localization of Ire1-mCherry and *PGK1*^{U1A} mRNA under normal (left panel, control) and ER stress (right panel, DTT) conditions. **g**, Localization of Lsm1-mCherry and *HAC1*^{U1A} mRNA without stress (left panel, control), after nutrient starvation for 10 min (middle panel, no glucose), or after induction of ER stress (right panel, DTT). **h**, **i**, Localization of Ire1-mCherry (red font), Ire1-GFP (green font), *HAC1*^{U1A}, or splicing reporter with 16 U1A hairpins as in *HAC1*^{U1A} (SpR^{U1A}) either with or without the $\Delta 3'$ BE deletion after induction of ER stress (DTT). **c**–**i**, ER stress was induced with 10 mM DTT for 45 min; imaging was performed in *ire1* Δ cells, complemented with Ire1 imaging constructs, except in **h** in which the cells were *hac1* Δ or *rlg1-100*, where indicated.

ref. 11), indicating that Ire1 oligomerization is the organizing principle for UPR signalling foci. Importantly, the inability of Ire1 to form foci impaired *HAC1*^{U1A} mRNA recruitment (Fig. 3f and Supplementary Fig. 3). Thus, when Ire1 fails to oligomerize, *HAC1* mRNA recruitment becomes rate limiting. In agreement, we found that artificially induced dimerization¹⁶ of Ire1 supported *HAC1* mRNA splicing and cell survival under ER stress conditions only to the level of the single-interface mutants and did not support Ire1 foci formation (Supplementary Fig. 4). We conclude that robust Ire1 oligomerization and *HAC1* mRNA targeting serve to concentrate both key UPR components into foci to ensure efficient RNA processing and ER stress signalling.

HAC1 mRNA is no longer a substrate for Ire1 after removal of its intron, indicating that the spliced *HAC1* mRNA should disengage from Ire1 foci and not be recruited again. Accordingly, SpR^{U1A} mRNA lacking the intron displayed reduced targeting to foci (CI: 17 ± 9) compared to wild-type SpR^{U1A} mRNA (Fig. 4a, b), although targeting was not as markedly reduced as when the 3' BE was deleted (Figs 2i and 4b). In further support, overexpression of SpR^{U1A} mRNA containing the intron reduced splicing of endogenous *HAC1* mRNA,

presumably by competitively saturating Ire1 after being targeted there, but did not do so when SpR^{U1A} mRNA lacked either the 3' BE or the intron (Fig. 4c). These observations indicate that the 3' BE alone is not sufficient for efficient targeting. In agreement, insertion of the 3' UTR stem of *HAC1* (Fig. 1c) into the 3' UTR of *PGK1* could not facilitate recruitment of this heterologous mRNA to Ire1 foci (Fig. 4d). Thus, the intron and 3' BE cooperate to effect *HAC1* mRNA targeting.

The intron keeps *HAC1* mRNA translationally silent (Fig. 1a), indicating that translational repression may be key to *HAC1* targeting similar to the situation in other mRNA targeting mechanisms, as observed for *ASH1* mRNA¹⁷. To test this hypothesis, we inserted a small stem-loop into the 5' UTR of the *PGK1*^{U1A} mRNA to repress its translation (ref. 17 and Fig. 4e). When we expressed *PGK1*^{U1A} mRNA containing both the small stem-loop in the 5' UTR and the *HAC1* 3' BE-containing stem in the 3' UTR, we found that this mRNA efficiently targeted to Ire1 foci (CI: 60 ± 19 , Fig. 4f, h). Conversely, the corresponding mRNA lacking the 3' BE was not targeted (Fig. 4g, h). We conclude that the 3' BE-containing stem is both necessary and sufficient to target a heterologous mRNA to UPR-induced Ire1 foci, provided that its translation is on hold. Translational repression,

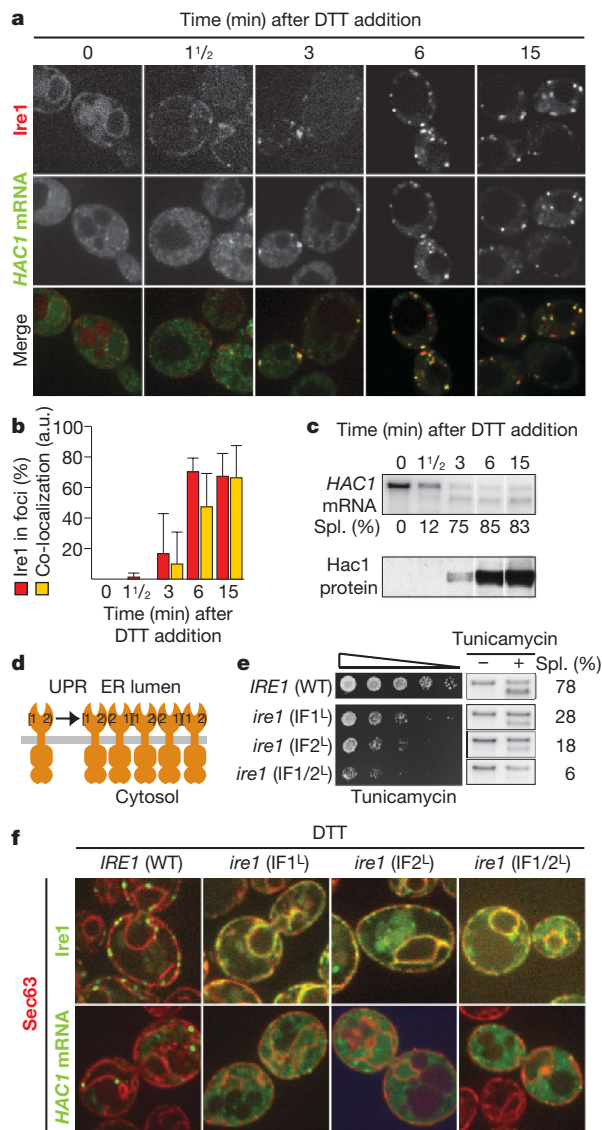


Figure 3 | The *HAC1* mRNA/*Ire1* foci are functional UPR signalling centres.

a, Localization of *Ire1*-mCherry and *HAC1*^{U1A} mRNA decorated with U1A-GFP. **b**, Quantification of the percentage of *Ire1* signal in foci (red bars) and of the co-localization index for *HAC1*^{U1A} mRNA recruitment into *Ire1* foci expressed in arbitrary units (yellow bars; means and s.e.m., $n = 5$). **c**, Northern blot of *HAC1* mRNA (top) and western blot of *Hac1* protein (bottom). **a–c**, Samples were taken at indicated times after induction of ER stress with 10 mM DTT. **d**, Schematic of *Ire1* oligomerization via interfaces 1 and 2. **e**, Viability assay under ER stress conditions ($0.2 \mu\text{g ml}^{-1}$ tunicamycin) and northern blot of *HAC1* mRNA collected from *ire1* Δ yeast complemented with wild-type *IRE1* or of *ire1* mutants that are defective in dimerization at luminal interface 1 (IF1^L), 2 (IF2^L) or both (IF1/2^L) before or after treatment with $1 \mu\text{g ml}^{-1}$ tunicamycin for 1 h. **f**, Localization of *Sec63*-mCherry, *Ire1*-GFP and *HAC1*^{U1A} mRNA. Imaging was performed in *ire1* Δ yeast complemented with wild-type or 'IF' mutants, either GFP-tagged (top) or untagged (bottom). ER stress was induced with 10 mM DTT for 45 min. Separate channels are displayed in Supplementary Fig. 3.

therefore, is not only key to facilitate timely synthesis of *Hac1* protein on induction of the UPR, but is also integral to the targeting of *HAC1* mRNA to ER stress signalling centres.

Our results describe the first example, to our knowledge, of mRNA targeting as a central feature in a signalling pathway. *HAC1* mRNA is delivered to the site where it is processed as part of the main switch regulating the UPR. The mRNA guidance mechanisms characterized so far serve other goals, such as delivery of mRNA to sites of storage or degradation^{18,19}, or restricted distribution of the proteins they encode^{20–22}. *HAC1* mRNA delivery to *Ire1* foci has in common with

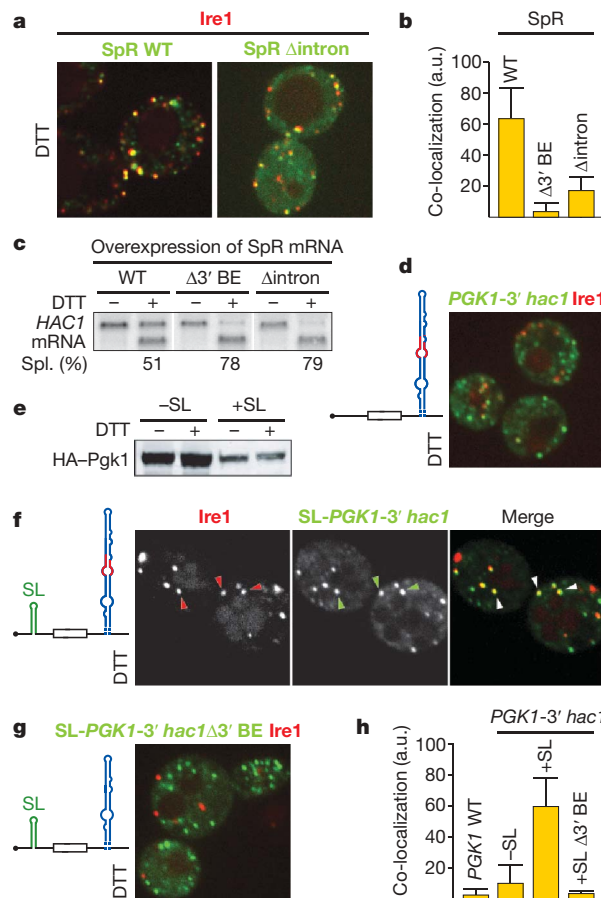


Figure 4 | Translational repression is a prerequisite for mRNA targeting to *Ire1* foci. **a, d, f, g**, Localization of *Ire1*-mCherry as well as either *SpR*^{U1A} mRNA (*SpR* WT), as in Fig. 2i, or an intron-less variant (*SpR* Δ intron, **a**), of *PGK1*^{U1A} bearing either the wild-type (*PGK1*-3'*hac1*, **d, f**) or the mutant Δ 3' BE (*PGK1*-3'*hac1* Δ 3' BE, **g**) 3' UTR stem-loop of *HAC1* mRNA, in combination with (**f, g**) or without (**d**) a small stem-loop (SL) that confers translational repression in its 5' UTR, as schematically depicted. **b**, Co-localization index for mRNA recruitment of WT and Δ intron splicing reporter variants into *Ire1* foci (means and s.e.m., $n = 5$); the bar for the Δ 3' BE mutant as depicted in Fig. 2i is shown for comparison. **c**, Northern blot of *HAC1* mRNA from yeast strains that overexpressed variants of the splicing reporter, as indicated. **e**, Western blot of the variants of HA-tagged *Pgk1* protein (HA-Pgk1) bearing the 3' UTR from *HAC1* with or without a 5' UTR stem-loop (SL). **a, c–g**, ER stress was induced with 10 mM DTT for 45 min. **h**, Co-localization index for mRNA recruitment into *Ire1* foci of *PGK1*^{U1A} wild type (see Fig. 2f) or variants shown in **d, f** and **g** (means and s.e.m., $n = 5–8$).

other mRNA-targeting mechanisms that it depends on a signal in the 3' UTR and on translational repression of the mRNA²³. The mechanism of translational control of *HAC1* mRNA serves both to prevent translation of a functional transcription factor when the UPR is off, and to allow the mRNA access to the splicing machine, which removes the intron to allow its translation, when the UPR is on. In this way, the targeting signal is inactivated when translation of *HAC1* mRNA resumes, even though the 3' BE remains present in the spliced mRNA.

The translational block in *Saccharomyces cerevisiae* is exerted by means of a 16-base-pairing interaction between sequences in the 252-nucleotide-long intron and the 5' UTR⁴. Most *HAC1* or *XBP1* orthologues bear introns that are shorter ($\sim 20–26$ nucleotides) and show no sequence complementarity to support 5' UTR/intron-based translational blocks. It is conceivable that other means of translational repression come into play. For instance, the general translational attenuation in response to ER stress as mediated by the ER-resident transmembrane eIF2 α kinase PERK²⁴ could serve a functionally similar role in *XBP1* mRNA targeting in metazoans.

Our findings emphasize the role of Ire1 oligomers, rather than dimers, in UPR signalling. Early co-immunoprecipitation studies already provided evidence for oligomerization²⁵, and the identification of two functionally important interfaces that link Ire1 luminal domains into linear filaments in the crystal lattice supports an attractive model by which neighbouring Ire1 molecules are 'stitched' together by the binding of unfolded proteins in the ER lumen¹⁵. This model and the epistasis data in Fig. 2h indicate that Ire1 foci formation is governed by self-organization. Overexpression of Ire1 caused an enlargement of the foci, but did not increase their number (not shown), indicating that there is a limited number of nucleation sites per cell and that foci may arise at such predisposed sites at the ER membrane. Because *HAC1* mRNA recruitment occurs with amazing speed and efficiency (for example, Fig. 3), one can further speculate that the 3' BE-containing targeting signal may allow *HAC1* mRNA to travel actively along cytoskeletal filaments to these pre-disposed sites, where Ire1 concentrates.

Clustering of activated signalling receptors occurs in many systems, such as in the immunological synapse²⁶ and in bacterial chemotaxis²⁷, and the resulting local concentration of the signalling machinery can greatly enhance the efficiency of signal transduction. Interestingly, we found that on oligomerization *in vitro* the nuclease activity of the Ire1 kinase/nuclease domains vastly increases²⁸ over the activity observed for Ire1 dimers²⁹. Thus, by clustering into oligomers, Ire1 acquires enhanced avidity towards its substrate *HAC1* mRNA and reaches full enzymatic activation at the same time. These mechanistic features converge into a signalling relay that provides the efficiency and time-liness required to combat ER stress.

METHODS SUMMARY

Microscopy data acquisition and analysis. Cells were visualized on a Yokogawa CSU-22 spinning disc confocal on a Nikon TE2000 microscope. Images of Ire1-mCherry and U1A-GFP-decorated *HAC1*^{U1A}, SpR^{U1A} and *PGK1*^{U1A} mRNAs and variants thereof were analysed using a customized MatLab script to determine the fraction of Ire1-mCherry in foci and to score the recruitment of U1A-GFP-decorated mRNA in Ire1 foci. The annotated MatLab script is available in the Supplementary Information. In brief, after background subtraction we defined the fraction of Ire1-mCherry in foci as the ratio between the integrated fluorescence intensity of pixels with a signal greater than a threshold value and the total integrated fluorescence intensity. The threshold was empirically defined such that under non-stress conditions no signal was scored as 'foci'. Similarly, RNA foci were defined as pixels exceeding by twofold the mean intensity in the RNA channel. A 'co-localization index' was then defined as the integrated intensity of the pixels within the RNA foci that had pixels in common with Ire1 foci divided by the total RNA intensity, and expressed in arbitrary units in a range from 0 to 100. For each condition, the percentage of Ire1-mCherry in foci and the co-localization index for the mRNA recruited to the foci was determined for 5–9 individual cells. Values and the standard error of the mean are given in histograms in Figs 2–4. Because, in contrast to the covalently fluorescently tagged Ire1, we do not know what fraction of U1A-GFP is bound to mRNAs containing U1A-binding sites, background subtraction for U1A-GFP was arbitrary. Therefore, we quantified the data by the co-localization index rather than an absolute percentage co-localization measure. The co-localization index robustly scores the differences in mRNA recruitment we observed qualitatively in the fluorescent micrographs.

Full Methods and any associated references are available in the online version of the paper at www.nature.com/nature.

Received 20 August; accepted 5 November 2008.

Published online 14 December 2008.

- Bernales, S., Papa, F. R. & Walter, P. Intracellular signaling by the unfolded protein response. *Annu. Rev. Cell Dev. Biol.* **22**, 487–508 (2006).
- Ron, D. & Walter, P. Signal integration in the endoplasmic reticulum unfolded protein response. *Nature Rev. Mol. Cell Biol.* **8**, 519–529 (2007).
- van Anken, E. & Braakman, I. Endoplasmic reticulum stress and the making of a professional secretory cell. *Crit. Rev. Biochem. Mol. Biol.* **40**, 269–283 (2005).
- Rüeggsegger, U., Leber, J. H. & Walter, P. Block of *HAC1* mRNA translation by long-range base pairing is released by cytoplasmic splicing upon induction of the unfolded protein response. *Cell* **107**, 103–114 (2001).

- Sidrauski, C., Cox, J. S. & Walter, P. tRNA ligase is required for regulated mRNA splicing in the unfolded protein response. *Cell* **87**, 405–413 (1996).
- Sidrauski, C. & Walter, P. The transmembrane kinase Ire1p is a site-specific endonuclease that initiates mRNA splicing in the unfolded protein response. *Cell* **90**, 1031–1039 (1997).
- Travers, K. J. *et al.* Functional and genomic analyses reveal an essential coordination between the unfolded protein response and ER-associated degradation. *Cell* **101**, 249–258 (2000).
- Gonzalez, T. N., Sidrauski, C., Dörfler, S. & Walter, P. Mechanism of nonsplicing mRNA splicing in the unfolded protein response pathway. *EMBO J.* **18**, 3119–3132 (1999).
- Brodsky, A. S. & Silver, P. A. Pre-mRNA processing factors are required for nuclear export. *RNA* **6**, 1737–1749 (2000).
- Diehn, M., Eisen, M. B., Botstein, D. & Brown, P. O. Large-scale identification of secreted and membrane-associated gene products using DNA microarrays. *Nature Genet.* **25**, 58–62 (2000).
- Kimata, Y. *et al.* Two regulatory steps of ER-stress sensor Ire1 involving its cluster formation and interaction with unfolded proteins. *J. Cell Biol.* **179**, 75–86 (2007).
- Bregues, M., Teixeira, D. & Parker, R. Movement of eukaryotic mRNAs between polysomes and cytoplasmic processing bodies. *Science* **310**, 486–489 (2005).
- Teixeira, D. & Parker, R. Analysis of P-body assembly in *Saccharomyces cerevisiae*. *Mol. Biol. Cell* **18**, 2274–2287 (2007).
- Ghaemmaghami, S. *et al.* Global analysis of protein expression in yeast. *Nature* **425**, 737–741 (2003).
- Credle, J. J., Finer-Moore, J. S., Papa, F. R., Stroud, R. M. & Walter, P. On the mechanism of sensing unfolded protein in the endoplasmic reticulum. *Proc. Natl Acad. Sci. USA* **102**, 18773–18784 (2005).
- Pollock, R. & Rivera, V. M. Regulation of gene expression with synthetic dimerizers. *Methods Enzymol.* **306**, 263–281 (1999).
- Chartrand, P., Meng, X. H., Huttelmaier, S., Donato, D. & Singer, R. H. Asymmetric sorting of Ash1p in yeast results from inhibition of translation by localization elements in the mRNA. *Mol. Cell* **10**, 1319–1330 (2002).
- Anderson, P. & Kedersha, N. RNA granules. *J. Cell Biol.* **172**, 803–808 (2006).
- Parker, R. & Sheth, U. P bodies and the control of mRNA translation and degradation. *Mol. Cell* **25**, 635–646 (2007).
- Kindler, S., Wang, H., Richter, D. & Tiedge, H. RNA transport and local control of translation. *Annu. Rev. Cell Dev. Biol.* **21**, 223–245 (2005).
- Choi, S. B. *et al.* Messenger RNA targeting of rice seed storage proteins to specific ER subdomains. *Nature* **407**, 765–767 (2000).
- Takizawa, P. A., DeRisi, J. L., Wilhelm, J. E. & Vale, R. D. Plasma membrane compartmentalization in yeast by messenger RNA transport and a septin diffusion barrier. *Science* **290**, 341–344 (2000).
- Czapinski, K. & Singer, R. H. Pathways for mRNA localization in the cytoplasm. *Trends Biochem. Sci.* **31**, 687–693 (2006).
- Harding, H. P., Zhang, Y. & Ron, D. Protein translation and folding are coupled by an endoplasmic-reticulum-resident kinase. *Nature* **397**, 271–274 (1999).
- Shamu, C. E. & Walter, P. Oligomerization and phosphorylation of the Ire1p kinase during intracellular signaling from the endoplasmic reticulum to the nucleus. *EMBO J.* **15**, 3028–3039 (1996).
- Bromley, S. K. *et al.* The immunological synapse. *Annu. Rev. Immunol.* **19**, 375–396 (2001).
- Maddock, J. R. & Shapiro, L. Polar location of the chemoreceptor complex in the *Escherichia coli* cell. *Science* **259**, 1717–1723 (1993).
- Korennykh, A. V. *et al.* The unfolded protein response signals through high-order assembly of Ire1. *Nature* doi:10.1038/nature07661 (this issue).
- Lee, K. P. *et al.* Structure of the dual enzyme Ire1 reveals the basis for catalysis and regulation in nonconventional RNA splicing. *Cell* **132**, 89–100 (2008).

Supplementary Information is linked to the online version of the paper at www.nature.com/nature.

Acknowledgements We thank M. Jonikas and B. Kornmann for their help with the MatLab scripts; R. Parker for the pPS2037 and pRP1187 plasmids; K. Thorn for the pKT127 plasmid and for his assistance with microscopy at the Nikon Imaging Center at UCSF; and C. Guthrie, R. Andino, J. Gross and members of the Walter laboratory for discussion and comments on the manuscript. T.A. was supported by the Basque Foundation for Science and the Howard Hughes Medical Institute; E.v.A. by the Netherlands Organization for Scientific Research (NWO); D.P. and C.A.R. by the National Science Foundation; C.A.R. by the President's Dissertation Year Fellowship; and A.V.K. by the Jane Childs Memorial Fund for Medical Research. P.W. is an Investigator of the Howard Hughes Medical Institute.

Author Contributions T.A. and E.v.A. wrote the manuscript, conceived the experiments and together with D.P. carried out most of the experimental work. I.M.S. and E.v.A. observed Ire1 foci, and C.A.R. performed all experiments concerning tRNA ligase localization. A.V.K. carried out kinetic analyses. P.W. directed the research programme and writing of the manuscript.

Author Information Reprints and permissions information is available at www.nature.com/reprints. Correspondence and requests for materials should be addressed to T.A. (Tomas.Aragon@ucsf.edu).

METHODS

Yeast strains and plasmids. Standard cloning and yeast techniques were used for construction, transformation and integration of plasmids^{30–32}. HA-tagged versions of *HAC1* with either its own 3' UTR or that of *ACT1* or *PGK1* were integrated as a genomic copy, replacing endogenous *HAC1*. The splicing reporter construct was generated by replacing positions 1 to 648 of the *HAC1* coding sequence in exon 1 with the GFP ORF. In the $\Delta 3'$ BE mutants, positions 176–182 and 212–218 of the 3' UTR of *HAC1* were deleted. The 3' BE stem that was placed between the stop codon and the *ACT1* 3' UTR of the splicing reporter comprised positions 155–187 and 207–236 of the 3' UTR of *HAC1*. The mRNA visualization constructs were created by inserting into the pRS426 vector³³ the sequences of *PGK1*, *HAC1* or a non-fluorescent GFP–R96A mutant of the splicing reporter ending at position 280 of the 3' UTR of *HAC1*, followed by 16 tandem repeats of the U1A binding sequence and the *PGK1* terminator, derived from pPS2037 (a gift from R. Parker), and a polyA signal. A copy of the U1A RNA-binding domain fused to GFP was integrated into the genome from plasmid pRP1187 (a gift from R. Parker). Surprisingly, the key to the low noise in the imaging lies in the curious fact that in pRP1187 the U1A–GFP ORF is inserted backwards, so that its expression is driven by a cryptic, uncharacterized promoter element within the (reverse) *PGK1* transcription terminator. The low levels of U1A–GFP expression derived from this construct prove ideal for mRNA imaging. By PCR, a previously described¹⁷ 5' stem-loop structure was introduced 26-nucleotides upstream of the start codon of *PGK1*, and nucleotides 108–280 of the *HAC1* 3' UTR, comprising the entire stem, were inserted after the *PGK1* stop codon, where indicated. A monomeric (A206R), yeast-codon-adapted version of GFP, derived from pKT127³⁴, or mCherry was placed into Ire1 between residues I571 and G572, and the FKBP-derived Fv2E domain (Ariad) between R112 and Y449, replacing the core ER-stress-sensing domain¹⁵. Ire1 luminal interface mutants are: IF1^L (T226W/F247A), IF2^L (W426A) and IF1/2^L (T226W/F247A/W426A)¹⁵. Ire1 variants in all assays were expressed at near-endogenous levels from centromeric pRS315.

RNA and protein analysis. RNA preparation, electrophoresis, labelling of probes for northern blot analysis and quantification of splicing efficiencies were performed as described⁴. Protein extraction, electrophoresis and transfer to nitrocellulose for immunoblot analysis with anti-HA antibody were performed as described⁴.

Microscopy. All samples were taken from yeast cells that were kept in early log phase for at least 24 h in synthetic media containing excess amounts of adenine and tryptophan before imaging. Light microscopy was done with a Yokogawa CSU-22 spinning disc confocal on a Nikon TE2000 microscope. GFP was excited with the 488 nm Ar-ion laser line and mCherry with the 568 nm Ar-Kr laser line. Images were recorded with a $\times 100/1.4$ NA Plan Apo objective on a Cascade II EMCCD. The sample magnification at the camera was 60 nm per pixel. The microscope was controlled with μ Manager and ImageJ. Images were selected

for analysis and for display in figures to contain no saturated pixels (in case of the RNA imaging) and a signal substantially above background (in case of Ire1–mCherry imaging). We excluded images of cells with strong vacuolar autofluorescence. Images were processed in ImageJ and Adobe Photoshop such that the linear range of the signal was comparable between images.

Quantitative analysis of Ire1 foci and co-localization of mRNA in foci. Images of Ire1–mCherry and U1A–GFP-decorated *HAC1*^{U1A}, SpR^{U1A} and *PGK1*^{U1A} mRNAs and variants thereof were analysed using a customized MatLab script to determine the fraction of Ire1–mCherry in foci and to score the recruitment of U1A–GFP-decorated mRNA in Ire1 foci. The annotated MatLab script is available (Supplementary Information). In brief, the mean pixel intensity of a background area ($\sim 20\%$ of section area) was defined in an intracellular area excluding ER. Ire1 was defined as all signal exceeding the mean background by 1.1-fold. Under non-stress conditions, we never observed this signal to exceed a 1.5-fold background threshold. We thus defined the fraction of Ire1 in foci as the ratio of Ire1–Cherry fluorescence intensity above threshold divided by the total Ire1–Cherry fluorescence intensity. The threshold was empirically defined such that under non-stress conditions no signal was scored as 'foci'. Similarly, RNA foci were defined as pixels exceeding by twofold the mean intensity in the RNA channel. A 'co-localization index' was then defined as the integrated intensity of the pixels within the RNA foci that had pixels in common with Ire1 foci divided by the total RNA intensity, and expressed in arbitrary units in a range of 0 to 100. For each condition, the percentage of Ire1–mCherry in foci and the co-localization index for the mRNA recruited to the foci was determined for 5–9 individual cells. Values and the standard error of the mean are given in histograms in Figs 2–4. Because, in contrast to the covalently fluorescently tagged Ire1, we do not know what fraction of the fluorescent reporter U1A–GFP in cells is bound to mRNAs containing U1A binding sites, background subtraction for U1A–GFP was arbitrary. Therefore, we report co-localization by this 'co-localization index' rather than by an absolute percentage co-localization measure. The co-localization index robustly scores the differences in mRNA recruitment we observed in the fluorescent micrographs.

30. Guthrie, C. & Fink, G. R. *Guide to Yeast Genetics and Molecular and Cell Biology* (Academic, 2002).
31. Longtine, M. S. *et al.* Additional modules for versatile and economical PCR-based gene deletion and modification in *Saccharomyces cerevisiae*. *Yeast* 14, 953–961 (1998).
32. Sambrook, J., Maniatis, T. & Fritsch, E. F. *Molecular Cloning: A Laboratory Manual* (Cold Spring Harbor Laboratory, 1989).
33. Sikorski, R. S. & Hieter, P. A system of shuttle vectors and yeast host strains designed for efficient manipulation of DNA in *Saccharomyces cerevisiae*. *Genetics* 122, 19–27 (1989).
34. Sheff, M. A. & Thorn, K. S. Optimized cassettes for fluorescent protein tagging in *Saccharomyces cerevisiae*. *Yeast* 21, 661–670 (2004).